The True Structure and Metal−Metal-Bonded Framework of $LiMo^{III}O_2$ Determined from Total Neutron Scattering

Simon J. Hibble,*,† Ian D. Fawcett,† and Alex C. Hannon‡

Department of Chemistry, University of Reading, Whiteknights, P.O. Box 224, Reading, RG6 6AD, U.K., and ISIS Facility, Rutherford Appleton Laboratory, Chilton, Didcot, Oxon OX11 0QX, U.K.

Received October 31, 1996[⊗]

Total neutron diffraction studies show that the layered lithium molybdate, $LiMo^{III}O_2$, contains zigzag molybdenum chains within the MoO_2 layers. The short distances along the zigzag, $d_{Mo-Mo} = 2.618$ Å, are indicative of strong metal−metal bonds. The structure adopted is in agreement with theoretical predictions for a d^3 metal system and differs from that previously published. The average structure is best described in the space group = $C2/m$, with $a = 10.543(6)$ Å, $b = 2.8626(5)$ Å, $c = 10.899(6)$ Å, and $\beta = 153.29(1)°$. The utility of determining radial correlation functions from diffraction data as a check on the final structure obtained from Bragg scattering studies of polycrystalline materials is demonstrated.

Introduction

Transition metal compounds containing MS_2 and MO_2 layers have attracted both technological and theoretical interest. Lithium intercalation compounds such as Li_xMX_2 (X = O or S) have been proposed as battery cathode materials.[1,2] The theoretical interest has lain in the electronic structure of the compounds and in the explanation of the structures adopted with different metal and d-orbital populations. An excellent summary of possible structural distortions is found in Burdett's book, *Chemical Bonding in Solids*.[3]

We became interested in $LiMoO_2$[4] as part of our reinvestigation of the structures of the lithium molybdates containing molybdenum in an oxidation state of IV and lower.[5] The published structure of $LiMoO_2$ by Aleandri and McCarley[4] contained undistorted hexagonal sheets, with each molybdenum surrounded by six close molybdenum neighbors at 2.87 Å, forming an infinite Mo−Mo-bonded hexagonal sheet, Figure 1a. This disagrees with accepted theoretical predictions for d^3 systems, which suggest that the structure would distort to allow the formation of either zigzag chains, Figure 1b, or diamond chain clusters, Figure 1c. Our Mo K-edge extended X-ray absorption fine structure studies (EXAFS)[5] showed that the published structure of $LiMoO_2$ was incorrect and that short metal−metal bonds of 2.56 and 2.71 Å were present rather than the shortest distances of 2.87 Å given in the published structure.[4] We concluded that our data favored the zigzag chain model but were unable to rule out other possible models such as the diamond chain found in ReS_2,[6] another d^3 system. In order to discriminate between the possible models for Mo−Mo bonding in $LiMoO_2$, we decided to carry out total neutron scattering studies in order to reinvestigate both the average structure responsible for Bragg scattering and to produce radial correlation functions to investigate the local structure in this material.

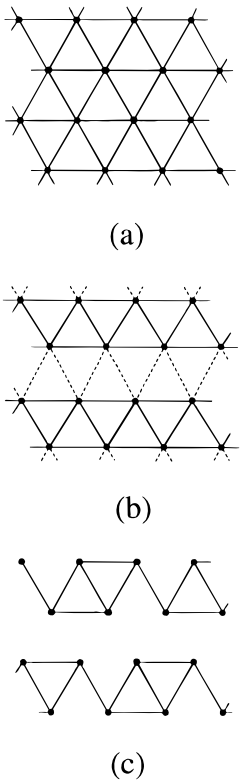

Figure 1. Some of the possible arrangements of metal ions in filled MoO_2 sheets: (a) Undistorted hexagonal molybdenum sheets; (b) zigzag clusters; (c) diamond chains.

Theory

The basic quantity measured in neutron diffraction is the differential cross section:[7]

$$d\sigma/d\Omega = I(Q) = I^s(Q) + i(Q) \quad (1)$$

where $I^s(Q)$ is known as the self-scattering and $i(Q)$ is known as the distinct scattering. Q is the magnitude of the scattering vector

† University of Reading.
‡ Rutherford Appleton Laboratory.
[⊗] Abstract published in *Advance ACS Abstracts,* April 1, 1997.

(1) Murphy, D. W; Christian, P. A. *Science* **1979**, *205*, 651.
(2) Jacobson, A. J. In *Intercalation Reactions of Layered Compounds* in *Solid State Chemistry Compounds*; Cheetham, A. K., Day, P., Eds.; Clarendon Press: Oxford, U.K., 1991.
(3) Burdett, J. K. *Chemical Bonding in Solids*; Oxford University Press: New York, 1995.
(4) Aleandri, L. E.; McCarley, R. E. *Inorg. Chem.* **1988**, *27*, 1041.
(5) Hibble, S. J.; Fawcett, I. D. *Inorg. Chem.* **1995**, *34*, 500.
(6) Murray, H. H.; Kelty, S. P, Chianelli, R. R. *Inorg. Chem.* **1994**, *33*, 4418.
(7) Wright, A. C. *Adv. Struct. Res. Diffr. Methods* **1974**, *5*, 1.

S0020-1669(96)01325-0 CCC: $14.00

(momentum transfer) for elastic scattering, given by

$$Q = \frac{4\pi \sin\theta}{\lambda} \tag{2}$$

After subtracting the self-scattering, the distinct scattering is Fourier transformed to give the total correlation function $T(r)$:

$$T(r) = T^{\circ}(r) + \frac{2}{\pi}\int_0^{\infty} Qi(Q)\, M(Q) \sin(rQ)\, dQ \tag{3}$$

$$T^{\circ}(r) = 4\pi r g^{\circ}(\sum_l c_l \bar{b}_l)^2 \tag{4}$$

where $M(Q)$ is a modification function (used to take into account that the diffraction pattern is measured up to a finite momentum transfer Q_{max} and not to infinity) and c_l is the atomic fraction for element l. The modification function is a step function cutting off at $Q = Q_{max}$, and the one used is that due to Lorch:[8]

$$M(Q) = \frac{\sin(Q\Delta r)}{Q\Delta r} \qquad \text{for } Q < Q_{max} \tag{5}$$

$$= 0 \qquad \text{for } Q > Q_{max} \tag{6}$$

where $\Delta r = \pi/Q_{max}$. $g^{\circ}(=N/V)$ is the macroscopic number density of the scattering units, n_l is the number of atoms of element l in the scattering unit, and $\bar{b}_l$ is the coherent neutron scattering length for element l.

To calculate $T(r)$ for our models, we employed the program XTAL[9] and the GENIE[10] input program RDF.[9] XTAL produced the partial pair distribution functions $g_{ll'}$ from the atomic and lattice parameters of our model

$$g_{ll'}(r) = \frac{1}{\sum_{i=1}^{N_l} w_i} \sum_{j=1}^{N_l}\sum_{\substack{j'=1 \\ j \neq j'}}^{N_{l'}} w_j w_{j'} \langle \delta(\boldsymbol{r} + \boldsymbol{R}_j - \boldsymbol{R}_{j'}) \rangle \tag{7}$$

where $\boldsymbol{R}_j$ is the position of the jth atom and w_i is the occupancy of the ith atom. The j,j' sums are over the $N_l,N_{l'}$ atoms of element l,l', and $j \neq j'$ means that j and j' are not allowed to refer to the same atom. $g_{ll'}$ may be interpreted as the number density of atoms of element l' at a distance r ($=|\boldsymbol{r}|$) from an origin atom of element l, averaged over all possible origin atoms and directions of $\boldsymbol{r}$. The weighted partial correlation functions $t_{ll'}$

$$t_{ll'}(r) = 4\pi g_{ll'}(r) \tag{8}$$

were then summed to yield the total correlation function $T(r)$:

$$T(r) = \sum_{ll'} c_l \bar{b}_l \bar{b}_{l'} t_{ll'}(r) \tag{9}$$

where c_l ($=N_l/N$) is the atomic fraction for element l, and $\bar{b}_l$ is the coherent neutron scattering length for element l, and the l and l' summations are both over the elements of the sample. The functions $t_{ll'}(r)$ and $T(r)$ were broadened using a Gaussian function to simulate the broadening of experimental data due to thermal motion and finite resolution in real space. This function

$$P(r) = \frac{1}{\sigma[2\pi]^{1/2}} \exp\left(\frac{(r - r_0)^2}{2\sigma^2}\right) \text{g} \tag{10}$$

preserved coordination numbers.

Experimental Section

Synthesis. Lithium Molybdates. $^7Li_2MoO_4$ was prepared by heating a mixture of $^7Li_2CO_3$ (99.95 at. % ^7Li) and MoO_3 (Aldrich, 99.5%) in the required stoichiometric quantities at 550 °C for 24 h in an alumina crucible. $^7LiMoO_2$ was prepared by heating together stoichiometric amounts of $^7Li_2MoO_4$ and Mo (Aldrich 99.95%) powder. The mixture was pressed into pellets and placed in an alumina crucible which was sealed in an evacuated silica tube. The reactants were heated at 500 °C for 24 h and then held at 900 °C for 4 days.

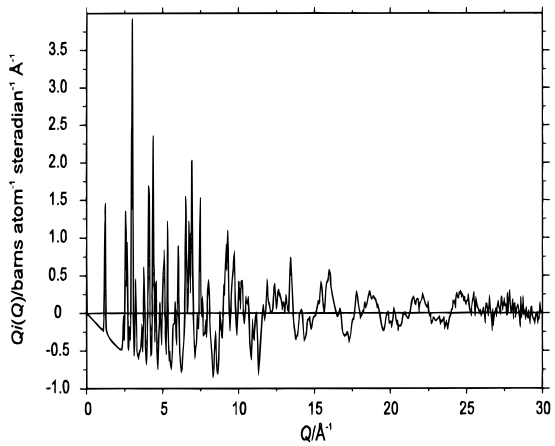

Figure 2. Interference function $Qi(Q)$ for $LiMoO_2$.

Sample Characterization. Powder X-ray diffraction patterns of the products were recorded using a Spectrolab Series 3000 CPS-120 X-ray diffractometer equipped with an INEL multichannel detector. The powder X-ray diffraction pattern for $LiMoO_2$ showed good overall agreement with a pattern calculated using the model of Aleandri and McCarley, but the c parameter was slightly larger. The lattice parameters, obtained by indexing on a hexagonal cell and calculated from the neutron data, are $a = 2.865(1)$ Å, $c = 15.6045(8)$ Å, for our sample, compared with those previously found by Aleandri and McCarley, $a = 2.8663(1)$ Å, $c = 15.4743(5)$ Å.[4]

Neutron Scattering Data Collection. Time of flight powder neutron diffraction data were collected on the LAD diffractometer at ISIS, Rutherford Appleton Laboratory, Chilton, Didcot, U.K.[11] LAD is equipped with pairs of detector banks at 5, 10, 20, 35, 58, 90, and 150°. A 5 g sample of powdered $^7LiMoO_2$ was loaded into a cylindrical 8 mm vanadium sample holder. The effective density of the sample, as used in the data correction routines, was determined from the sample depth. The sample was cooled to 12−13 K using a closed cycle refrigerator. Data were collected over the time of flight range, 100−19 750 μs (Q range, 0−50 Å^{-1}). Background runs were collected on the empty can and empty spectrometer, and data were collected for a standard vanadium rod.

Data Reduction and Analysis. (a) Rietveld Analysis. Data for Rietveld analysis were obtained by combining the signals from the two 150° detector banks and normalizing to the neutron flux. Standard Rietveld refinements for $^7LiMoO_2$ were carried out using the program TF12LS,[12] over the d-space range 0.46−3.55 Å, with the peak shape modeled by a pseudo-Voigt function convoluted with a double exponential function. The coherent scattering lengths used for ^{7}Li, Mo, and O were -0.22×10^{-14}, 0.69×10^{-14}, and 0.5805×10^{-14} m, respectively.[13]

(b) Total Neutron Scattering. Data for total neutron scattering were obtained by merging the data from all 14 detector banks (over the Q range 0−30 Å^{-1}), normalized to absolute scattering units, after correcting for detector dead time, multiple scattering, inelasticity, and attenuation using the ATLAS suite of programs.[14]

The interference function, $Qi(Q)$, for $^7LiMoO_2$, out to $Q = 30$ Å^{-1}, is shown in Figure 2.

(8) Lorch, E. *J. Phys.* **1969**, *C2*, 229−237.
(9) Hannon, A. C. *Rutherford Appleton Laboratory Report, RAL-93-063*; Rutherford Appleton Laboratory: Didcot, U.K., 1993.
(10) David, W. I. F.; Johnson, M. W.; Knowles, K. J.; Moreton-Smith, C. M.; Crosbie, G. D.; Campbell, E. P.; Graham, S. P.; Lyall, J. S. *Rutherford Appleton Laboratory Report, RAL-86-102*; Rutherford Appleton Laboratory: Didcot, U.K., 1986.
(11) Howells, W. S. *Rutherford Appleton Laboratory Report, RAL-80-017*; Rutherford Appleton Laboratory: Didcot, U.K., 1980.
(12) David, W. I. F.; Ibberson, R. M.; Matthewman, J. C. *Rutherford Appleton Laboratory Report, RAL-92-032*; Rutherford Appleton Laboratory: Didcot, U.K., 1992.
(13) Koester, L.; Yelon, W. B. *Summary of Low Energy Neutron Scattering Lengths and Cross Sections*; Department of Physics, Netherland Research Foundation: Petten, The Netherlands, 1982.
(14) Soper, A. K.; Howells, W. S.; Hannon, A. C. *Rutherford Appleton Laboratory Report, RAL-89-046*; Rutherford Appleton Laboratory: Didcot, U.K., 1989.

Table 1. Refined Atomic Parameters for $LiMoO_2$ (Space Group $R\bar{3}m$; Hexagonal Mo Sheets) with Estimated Standard Deviations in Parentheses[a]

atom	site	*x*	*y*	*z*	B/Å^2
Mo	3a	0	0	0	1.32(6)
Li	3b	0	0	$^1/_2$	1.1(1)
O	6c	0	0	0.2532(2)	0.50(3)

[a] Space group = $R\bar{3}m$, a = 2.865(1) Å, c = 15.6045(8) Å. (1) Rietveld fit: number of reflections used = 180, $\chi^2 = (R_{wp}/R_{ex})^2 = 1198$ for 2541 observations and 16 basic variables, $R_{wp} = [\Sigma_i w_i|Y_i(\text{obs}) - Y_i(\text{calc})|^2/\Sigma_i w_i Y_i(\text{obs})^2]^{1/2} = 0.1212$, $R_{ex} = [(N - P + C)/\Sigma_i w_i Y_i(\text{obs})^2]^{1/2} = 0.0035$; R_{wp} is the weighted profile R factor, R_{ex} is the expected R factor, w_i is the weight for point i, N = number of observations, Y_i is the intensity of point i, P = number of variables, and C = number of constraints. (2) Fit to $T(r)$: $R_{T(r)} = [\Sigma_i|Y_i(\text{obs}) - Y_i(\text{calc})|^2/\Sigma_i Y_i(\text{obs})^2]^{1/2}$ (over the fit range 1.5−7.0 Å) = 0.378.

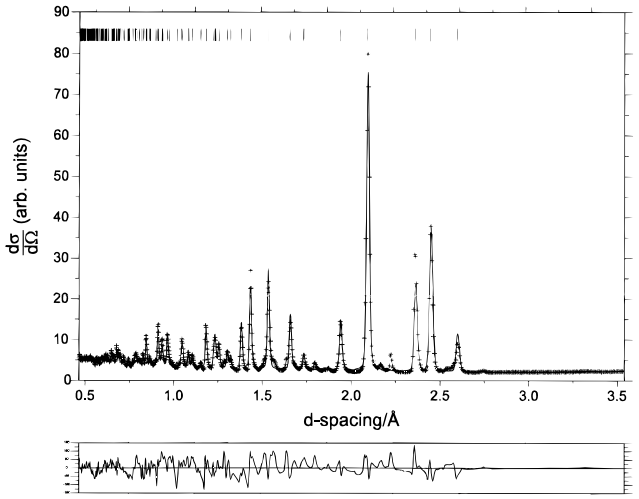

Figure 3. Final fitted profiles (points, observed; line, calculated; lower, difference) from Rietveld refinements for $LiMoO_2$ using the Aleandri and McCarley model in space group $R\bar{3}m$. Marks directly above the diffraction pattern indicate positions of allowed reflections.

Modeling, Results, and Discussion

Aleandri and McCarley's model for $LiMoO_2$[4] in space group $R\bar{3}m$ was used as a starting point for the Rietveld refinements. The scale and five polynomial background parameters were refined first, followed by the unit cell, the atomic parameters, the independent temperature factors, and finally the peak parameters. The refined lattice and atomic parameters are given in Table 1, and I_{obs}, I_{calc}, and the difference plots are shown in Figure 3. We found reasonable agreement with the results of Aleandri and McCarley. The oxygen *z* parameters are in good agreement, having values of 0.2532 and 0.2548 respectively for our work and theirs, but our atomic temperature factors are smaller and our lattice parameter is slightly larger (0.83%) than theirs, and that found for our EXAFS sample.[5] Part of the difference arises from the fact that our experiments were carried out at 13 K rather than 300 K, but the difference in the lattice parameter is significant and discussed later. The lower temperature factors are as would be expected, but detailed interpretation is difficult since they contain a contribution from both thermal and static disorder. Temperature factors are difficult to interpret in disordered materials. It is clear from Figure 3 that the structure refinement gives rather a poor fit to the experimental data. An impurity peak from molybdenum metal can be seen at d = 2.23 Å, but the overall quality of the data appears to be higher than that of Aleandri and McCarley, who had problems with significant quantities of Li_2MoO_4 in their sample. The contribution to the total scattering from molybdenum metal is small (<2%), and no real improvement is made to the refinement by excluding peaks due to it. The extremely high χ^2 for our study is a result of the long counting time and resulting high intensities which are necessary for analysis of total scattering, these lead to very small expected statistical errors and the low expected *R*-factor. The quality of agreement of the observed and calculated profiles shows that problems remain in describing this structure. This is not surprising, since we knew from our EXAFS study[5] that this model did not accurately describe the metal−metal-bonded clusters in this material.

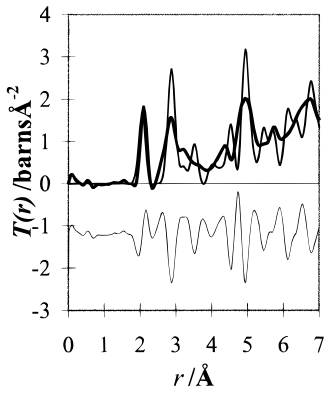

Figure 4. Experimentally determined radial correlation function, $T(r)_{exp}$, for $LiMoO_2$, shown with a heavy line, and the calculated, $T(r)_{calc}$, shown with a light line for the structure in space group $R\bar{3}m$.The difference plot is shown below the line.

A much more revealing indication of problems with the structural model can be seen in the radial correlation function derived from total neutron scattering. The total correlation function, $T(r)$, from 0 to 7 Å, obtained by Fourier transforming $Qi(Q)$ according to eq 3 for $^7LiMoO_2$, is shown in Figure 4 together with that calculated from the positional parameters of the average structure given in Table 1, using a value of σ = 0.1 Å to account for thermal and resolution broadening of $T(r)$. Figure 4 shows clearly that the short and medium range structure in $LiMoO_2$ is poorly modeled by the structural model given in Table 1 and yields an $R_{T(r)}$ factor of 0.378 over the fit range of 1.5−7.0 Å. This disagreement was not unexpected, since we knew from EXAFS studies[5] that these materials contained metal−metal-bonded clusters not included in the average structure.

In an attempt to produce a better model to describe the structure of $LiMoO_2$, we looked at the structures of related materials. The sodium molybdates, Na_xMoO_2,[15] and the lithium molybdate, $Li_{0.74}MoO_2$,[4,16] all contain zigzag molybdenum chains, in agreement with theoretical predictions for d^{3-4} systems. A model based on the structure of $Li_{0.74}MoO_2$, space group $C2/m$, derived from the single crystal X-ray diffraction data supplied by McCarley,[16] gave a much improved fit to $T(r)$, and we then used this as a starting point for a Rietveld refinement. The refinement was carried out in the same way as that for the model in $R\bar{3}m$. The refined lattice and atomic parameters are given in Table 2; I_{obs}, I_{calc}, and the difference plots are shown in Figure 5. Table 3 gives selected interatomic distances for this model and compares them with those found from EXAFS and from the refinement in space group $R\bar{3}m$, and Figure 6 shows the structure. The refinement gave a slight improvement in fit measured by the various *R*-factors. Careful inspection shows that a number of weak peaks unaccounted for by the model in $R\bar{3}m$ are now fitted, for example the small peak at d = 2.75 Å. These peaks could easily be missed or ascribed to impurities in a powder diffraction study.

(15) McCarley, R. E; Lii, K.-H.; Edwards, P. A.; Brough, L. F. *J. Solid State Chem.* **1985**, *57*, 17.
(16) McCarley, R. E. Personal communication, 1996.

Table 2. Refined Atomic Parameters for $LiMoO_2$ (Space Group *C*2/*m*; Zigzag Molybdenum Chain Model) with Estimated Standard Deviations in Parentheses[a]

atom	site	*x*	*y*	*z*	*B*/Å^2
Mo	4i	0.4701(9)	0	0.2210(9)	0.93(5)
O1	4i	0.248(1)	0	0.867(1)	0.45(2)
O2	4i	0.755(1)	0	0.615(1)	0.45(2)
Li1	2c	$^1/_2$	$^1/_2$	$^1/_2$	1.8(1)
Li2	2a	0	0	0	1.8(1)

[a] Space group = *C*2/*m*, a = 10.543(6) Å, b = 2.8626 (5) Å, c = 10.899(6) Å, b = 153.29(1)°. (1) Rietveld fit: number of reflections used = 857, χ^2 = 756 for 2541 observations and 23 basic variables, R_{wp} = 0.0963, R_{ex} = 0.0035. (2) Fit to *T(r)*: $R_{T(r)}$ = 0.122 (*R*-factors defined in Table 1).

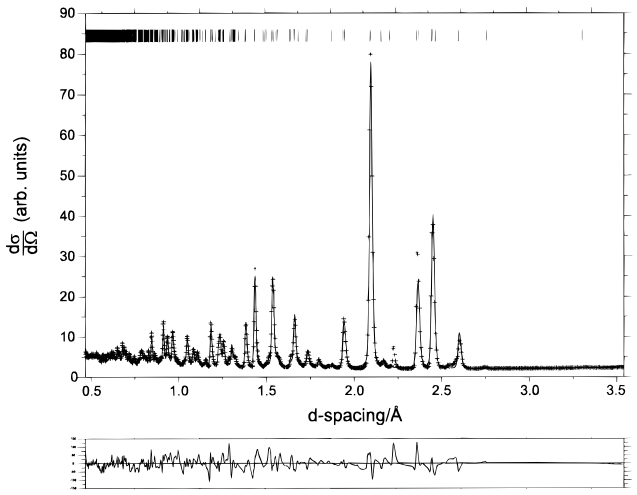

Figure 5. Final fitted profiles (points, observed; line, calculated; lower, difference) from Rietveld refinements for $LiMoO_2$ using the *C*2/*m* model. Marks directly above the diffraction pattern indicate positions of allowed reflections.

Table 3. Selected Interatomic Distances (Å) in $LiMoO_2$ (*C*2/*m* Structure) Compared to Those from EXAFS and the Average Structure in $R\bar{3}m$

	neutron scattering *C*2/*m*	EXAFS	neutron scattering $R\bar{3}m$
Mo−Mo	2.617 (×2)	2.561 (×2)	
	2.863 (×2)	2.709 (×2)	2.865 (×6)
	3.122 (×2)	3.162	
Mo−O(1)	2.056		
	2.078 (×2)	2.024 (×6)	2.135 (×6)
Mo−O(2)	2.094 (×2)		
	2.102		

A still more revealing measure of the superiority of the new structural model can be seen by examining the fit of the theoretical $T(r)_{calc}$, produced using the positional parameters in Table 2 and an overall σ of 0.1 Å to account for thermal and resolution broadening, to the experimental radial correlation function $T(r)_{exp}$, derived from total neutron scattering. This is shown in Figure 7. The new model in space group *C*2/*m* clearly gives a much improved fit; this is reflected in the $R_{T(r)}$ factor of 0.122 compared to 0.378 for the model in $R\bar{3}m$. Although the fit to the medium range order in $LiMoO_2$ is good, the *R*-factors for the Rietveld refinement remain high. A likely reason for this is disorder in the material in the form of stacking faults. This would account for difficulties in modeling the peak shapes and remaining discrepancies in the Rietveld refinement. There is a very simple mechanism for allowing stacking disorder in this material, in consequence of the near equality of twice the repeat distance along the horizontal straight boundary of the zigzag chain shown in Figure 1b and the diagonal Mo−Mo···-Mo distance. These two distances are found to be 5.725 and 5.739 Å, respectively, in $LiMoO_2$. It is easy to envisage rotating one MO_2 layer by 120° with respect to an adjacent layer. These layers would grow epitaxially one upon the other. The zigzag chains in one layer would now run at 120° relative to those in the adjacent layer. Figure 8 shows the relative arrangement of the metal chains in two such layers. Only a small amount of disruption would occur in the coordination sphere of the lithium atoms, which bind the MoO_2 layers together. The rotation

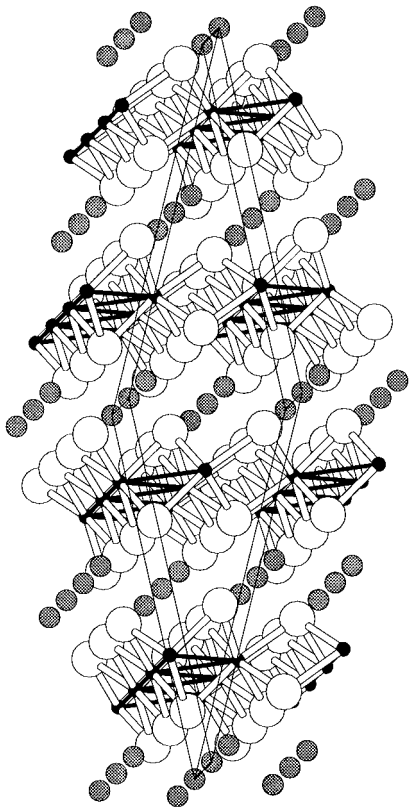

Figure 6. Final structural model for $LiMoO_2$ as seen along the *b* axis (solid circles, Mo; open circles, O; lightly shaded circles, Li). Light lines indicate the unit cell.

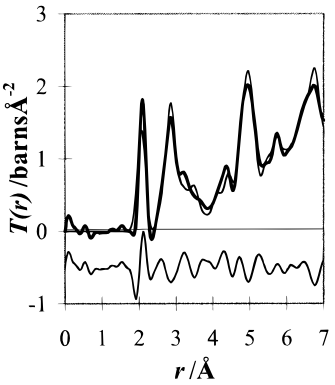

Figure 7. Experimentally determined radial correlation function, $T(r)_{exp}$, for $LiMoO_2$, shown with a heavy line, and the calculated, $T(r)_{calc}$, shown with a light line, for the structure in space group *C*2/*m*. The difference plot is shown below the line.

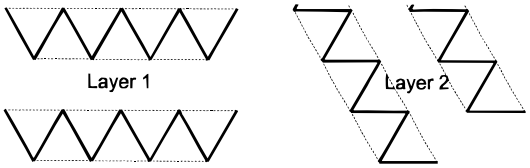

Figure 8. Possible mechanism for disorder in $LiMoO_2$: Mo−Mo-bonded chains rotated by 120° in adjacent MoO_2 layers.

would simply interchange O(1) and O(2) atoms in one of the triangular faces of the near octahedral coordination sphere of the lithium atoms and lead to only minor changes in coordination geometry.

The remaining fact to be accounted for is the difference between the hexagonal lattice parameters found by Aleandri and McCarley for $LiMoO_2$, $a = 2.8663(1)$ Å, $c = 15.4743(5)$ Å,[4] and those found in this work, $a = 2.865(1)$ Å, $c = 15.6045(8)$ Å. A possible explanation for this can be found by considering the $Li_2O-Mo-MoO_3$ phase diagram. We found two compounds on the Li_2O-MoO_2 tie line, Li_2MoO_3, which was known previously, and $Li_4Mo_3O_8$.[5] These two compounds and $LiMoO_2$ have closely related structures, and a notable feature is that the cell metrics of $LiMoO_2$ and $Li_4Mo_3O_8$ differ very little, <0.2% for *a* and 1−2% for *c* depending on preparation. Aleandri and McCarley prepared their $LiMoO_2$ in the presence of excess Li_2MoO_4 at 900 °C. We made $Li_4Mo_3O_8$, which lies on the $Li_2MoO_4-LiMoO_2$ tie line, at 750 °C. It would therefore appear that $Li_4Mo_3O_8$ is not stable at 900 °C. These facts, however, suggest that a possible explanation for the variation in lattice parameters for "$LiMoO_2$" samples is that intergrowths of $Li_4Mo_3O_8$ can occur in $LiMoO_2$ at high temperature. Dissolving a small amount of $Li_4Mo_3O_8$ in $LiMoO_2$ would affect the lattice parameters and the long-range order in the material. The $Li_2O-Mo-MoO_3$ phase diagram appears to have a yet deeper level of complication which we have just begun to touch upon!

Conclusions

Total neutron scattering studies have allowed us to determine the correct metal−metal-bonded framework in $LiMoO_2$. We have shown that modeling radial correlation functions is an extremely useful check on the correctness of a structure determination. The fit to *T(r)* can be much more sensitive to structural model deficiencies than the fit to Bragg scattering. This is illustrated in this paper by the demonstration that an apparently reasonable model for $LiMoO_2$, determined from Bragg diffraction data and refined by Rietveld methods, is obviously incorrect when the calculated *T(r)* is compared with *T(r)* determined from total neutron scattering. The improvement in the *R*-factor for the fit of the *T(r)* data, from 0.378 to 0.122, is much greater than the improvement from 0.1212 to 0.0963 in R_{wp} for the Rietveld refinement, when moving from the incorrect to correct structure. This method can clearly be extended to other polycrystalline materials and is extremely useful where underlying disorder can cause difficulties in describing the Bragg peak shapes.

Acknowledgment. We thank the EPSRC for the provision of neutron diffraction facilities and a studentship for I.D.F. and R. E. McCarley for providing us with unpublished single crystal data for $Li_{0.74}MoO_2$.

Supporting Information Available: Listings of intensity against d-spacing, the data used in the Rietveld refinement, and of *i(Q)* against *Q*, the data used in the radial distribution calculation (16 pages). Ordering information is given on any current masthead page.

IC961325C